Membrane Interactions of Novicidin, a Novel Antimicrobial Peptide: Phosphatidylglycerol Promotes Bilayer Insertion

Jerzy Dorosz,[†,‡] Yana Gofman,[§,||] Sofiya Kolusheva,[†] Daniel Otzen,[⊥] Nir Ben-Tal,[||] Niels Chr. Nielsen,[‡] and Raz Jelinek*[,†]

Department of Chemistry and Ilse Katz Institute for Nanotechnology, Ben Gurion University, Beer Sheva 84105, Israel, Center for Insoluble Protein Structures (inSPIN), Interdisciplinary Nanoscience Center (iNANO) and Department of Chemistry, Aarhus University, DK-8000 Aarhus C, Denmark, GKSS Research Center, Geesthacht 21502, Germany, Department of Biochemistry and Molecular Biology, The George S. Wise Faculty of Life Sciences, Tel Aviv University, Ramat Aviv 69978, Israel, and Center for Insoluble Protein Structures (inSPIN), Interdisciplinary Nanoscience Center (iNANO) and Department of Molecular Biology, Gustav Wieds Vej 10C, Aarhus University, DK-8000 Aarhus C, Denmark

Received: June 7, 2010; Revised Manuscript Received: July 22, 2010

Novicidin is an antimicrobial peptide derived from ovispirin, a cationic peptide which originated from the ovine cathelicidin SMAP-29. Novicidin, however, has been designed to minimize the cytotoxic properties of SMAP-29 and ovisipirin toward achieving potential therapeutic applications. We present an analysis of membrane interactions and lipid bilayer penetration of novicidin, using an array of biophysical techniques and biomimetic membrane assemblies, complemented by Monte Carlo (MC) simulations. The data indicate that novicidin interacts minimally with zwitterionic bilayers, accounting for its low hemolytic activity. Negatively charged phosphatidylglycerol, on the other hand, plays a significant role in initiating membrane binding of novicidin, and promotes peptide insertion into the interface between the lipid headgroups and the acyl chains. The significant insertion into bilayers containing negative phospholipids might explain the enhanced antibacterial properties of novicidin. Overall, this study highlights two distinct outcomes for membrane interactions of novicidin, and points to a combination between electrostatic attraction to the lipid/water interface and penetration into the subsurface lipid headgroups region as important determinants for the biological activity of novicidin.

1. Introduction

Antimicrobial peptides (AMPs) are essential components of innate immunity in multicellular organisms due to their selectivity and rapid response, crucial for encountering the fast proliferation of microorganisms.[1–3] Studying and developing new AMPs has become particularly important in the light of the emergence of antibiotic-resistant bacterial strains. Although these peptides display high amino-acid sequence diversity, they generally encompass short peptides (12−60 residues),[4] and seem to possess two common characteristics: amphiphilicity (approximately 50% hydrophobic residues) and net positive charge (2−9 lysine or arginine residues).[5] Many AMPs do not exhibit ordered structures in water; however, they adopt specific secondary structures in membrane environments, a transformation that is believed to be a major factor in their antimicrobial activity.[6] However, in a recent work on antimicrobial peptide mimics,[7] the requirement of a defined secondary structure as a critical factor of antimicrobial activity has been challenged.

Numerous studies have aimed to decipher the modes of action of AMPs and their specificity for bacterial cells rather than host cells.[8,9] The amphiphilic properties of AMPs generally enhance their affinity to lipid membranes, which are believed to be their initial, and most likely primary targets.[9] In particular, the positive charge of AMPs is believed to contribute to peptide specificity toward *bacterial* membranes, which are enriched in anionic lipids, in contrast to the more neutral surfaces of mammalian cells.[1,8,9]

Antimicrobial peptides have been shown to form membrane pores, which are believed to cause leakage of important metabolites and lead to bacterial cell death. Two different types of membrane pores have been described, namely, a barrel-stave pore (observed for alamethicin), where the pore is lined solely with the peptide,[10,11] and a toroidal pore (for many helical, amphipathic peptides such as magainin) in which the peptide induces a curvature in the membrane and the pore is lined with both peptide and lipids.[12,13] Dermaseptin on the other hand has been shown to self-associate in the presence of anionic lipids, forming a "carpet" at the membrane's surface, which breaks after the peptide reaches a critical concentration.[11]

A more general description has been proposed by Huang et al.,[14] according to which a peptide can exist in one of two possible states: inactive, parallel to the membrane surface and active, transmembrane state, depending on the relative peptide/lipid proportion in the membrane. For lower peptide/lipid ratios, the energetically favored orientation is parallel to the membrane and the peptide is embedded on the interface region between hydrophobic acyl chains and hydrophilic lipid headgroups. At

* To whom correspondence should be addressed. E-mail: razj@bgu.ac.il. Phone: +972-8-6428665. Fax: +972-8-6472943.
[†] Ben Gurion University.
[‡] Center for Insoluble Protein Structures (inSPIN), Interdisciplinary Nanoscience Center (iNANO) and Department of Chemistry, Aarhus University.
[§] GKSS Research Center.
[||] Tel Aviv University.
[⊥] Center for Insoluble Protein Structures (inSPIN), Interdisciplinary Nanoscience Center (iNANO) and Department of Molecular Biology, Aarhus University.

10.1021/jp1052248
Published on Web 08/06/2010

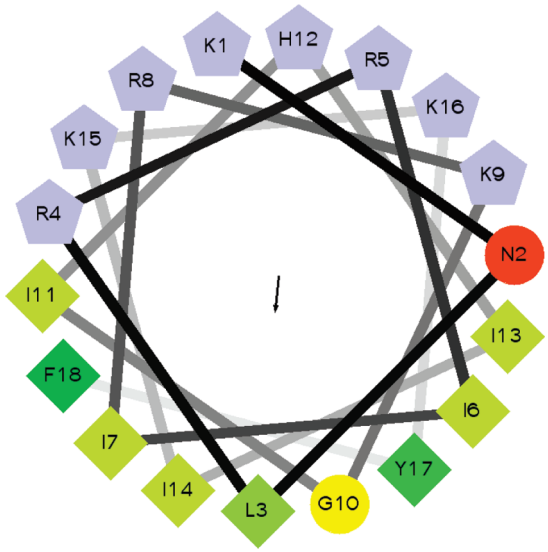

Figure 1. Helical wheel projection of novicidin. All lysine and arginine residues (gray color) are located at one side of the amphipathic helix, whereas the hydrophobic residues (yellow-green color) are facing the opposite side. The vector in the middle of the wheel represents the hydrophobic moment of the molecule. The image was created using wheel.pl software, version 1.4.

higher peptide/lipid ratios, a transmembrane orientation is preferred which allows the peptide to assemble and to form oligomeric pores. Another proposed model for AMP action—the "detergent-like" model—takes into account the geometry of the lipid molecules intercalated by an amphiphilic peptide which induces a curvature strain in the lipid bilayer, therefore acting like a detergent molecule and disrupting the membrane.[15] Recent nuclear magnetic resonance (NMR) and molecular dynamics (MD)-based studies of alamethicin in phospholipid bilayers, micelles, and bicelles[16,17] indicate that AMPs display a very high degree of flexibility in their membrane binding conformations which may be important for different modes of action.

Ovispirin is a synthetic peptide derived from the N-terminus of the sheep cathelicidin SMAP-29.[18,19] Ovispirin (sequence KNLRRIIRKIIHIIKKYG) is highly cytolytic, and thus, its applicability as a potential AMP is limited.[18] This observation has prompted an effort by Novozymes A/S to develop peptide variants with reduced activity toward mammalian cells. A double amino acid substitution I10G and G18F produced *novicidin*, a peptide displaying a favorable combination of effective antimicrobial activity and low hemolytic properties. Assuming the peptide adopts an ideal α-helical structure, the distribution of positively charged and hydrophobic residues in the sequence results in a highly amphipathic structure (Figure 1). The helical-wheel representation of novicidin suggests a high affinity of the peptide to anionic lipids that could counterbalance the repulsion of positively charged residues, and points to an interesting profile of membrane interactions. Here, we present a comprehensive investigation of the biological activity and membrane interactions of novicidin, with the goal of shedding light upon its cell selectivity and mechanism of action.

2. Materials and Methods

2.1. Materials. Novicidin was generously provided by Dr. Hans Henrik Kristensen (Novozymes A/S).

Melittin was purchased from Sigma-Aldrich. All phospholipids, including 1,2-dimyristoyl-*sn*-glycerophosphocholine (DMPC), 1,2-dimyristoyl-*sn*-glycero-3-phospho-(1′-*rac*-glycerol) (DMPG) sodium salt, and ESR probe 1-palmitoyl-2-stearoyl-(10-*doxyl*)-*sn*-glycero-3-phosphocholine, were purchased from Avanti Polar Lipids, Inc. (Alabaster, AL). Stock solutions (40 and 20 mM for DMPC and DMPG, respectively) were prepared by dissolution of the phospholipids in chloroform:ethanol 1:1 mixtures, and were kept at −20 °C. For monolayer experiments, phospholipid stock solutions of 1 mM were used. Stock solution of the ESR probe was prepared by dissolution in ethanol to a final concentration of 1 mg/mL and stored at −20 °C.

The diacetylene monomer 10,12-tricosadiynoic acid was obtained from Alpha Aesar, Lancaster Synthesis (Lancashire, England). 60 mM stock solution was prepared by dissolution of 10,12-tricosadiynoic acid in chloroform:ethanol mixture and stored at −20 °C.

2.2. Hemolysis Assay. 1 mL of fresh blood from a human donor was centrifuged at 4000*g* to separate erythrocytes from blood plasma. Erythrocytes were washed four to five times with PBS and centrifuged at 4000*g*, until no trace of free hemoglobin was visible in the supernatant. The pellet of red blood cells was resuspended in 10 mL of PBS (therefore diluting the initial portion of erythrocytes 10 times) and treated with a range of 2-fold dilutions of novicidin and melittin and incubated for 30 min at 37 °C with gentle shaking (100 rpm). As a positive control (100% lysis), we used a sample treated with 1% Triton X100. The suspension was centrifuged (4000*g*) to separate intact red blood cells from the supernatant. The amount of free hemoglobin in the supernatant was determined by measuring the absorbance at 560 nm. Each experiment comprised two *independent* measurements, and the experiments were repeated twice. These four measurements were the basis for the calculation of SD.

2.3. Antibacterial Assay. Three different bacteria strains were used to determine the killing efficiency of the novicidin: *Escherichia coli* BL21 and *Salmonella enterica ser. typhimurium* (Gram-negative) and *Bacillus cereus* wild type (Gram-positive). Bacteria were cultured at 37 °C in LB medium to reach an optical density of 0.4−0.6 at 560 nm (midlog phase) and then diluted 1000 times and subsequently transferred to a 96-well microplate (Greiner) followed by treatment with a range of 2-fold dilutions of antimicrobial substances: two highly positively charged peptides (novicidin and bee-venom-derived melittin) and a conventional antibiotic (streptomycin). Bacteria were incubated at 37 °C for 16 h (overnight) with shaking (200 rpm). After incubation, the optical density (at 560 nm) was measured to estimate the growth inhibition. The MIC 50 was a concentration, which caused a decrease of optical density by 50% compared with the control. The experiment comprised two independent measurements, and was repeated two times, yielding a mean value ± SD.

2.4. Monolayer Adsorption Experiments. The experiments were performed at 25 °C using a Nima 312D Teflon trough (Nima Technology Ltd., Coventry, U.K.). The absorption isotherms ($\Delta\pi$−time) were monitored throughout the duration of the experiment using a Nima PS4, Wilhelmy plate sensor. Lipid monolayers at different surface pressures were formed by deposition of the lipid solutions at the air−water interface of the dipping well (total volume of 50 mL). After 15 min of solvent evaporation and equilibration, the peptide was injected into the water subphase, below the preformed lipid monolayer through a thin, vertical tube, to reach 200 ng/mL (87 nM) concentration followed by 2−3 h of incubation with gentle stirring.

2.5. Lipid Vesicle Preparation. Phospholipid stock solutions in chloroform:ethanol 1:1 mixture were transferred to a glass

tube and evaporated under vacuum for several hours. In the liposomes for ESR experiments, the doxyl probe (1-palmitoyl-2-stearoyl-(10-*doxyl*)-*sn*-glycero-3-phosphocholine) constituted 2% of all lipids (molar ratio). The lipid film formed on a glass surface was hydrated by incubation in Tris buffer for a few minutes followed by probe sonication on a Misonix Incorporated sonicator (Farmingdale, NY). The suspensions were incubated at room temperature for 60 min and centrifuged at 5000*g* to remove titanium particles.

2.6. Polydiacetylene (PDA)/Phospholipid Vesicles. 10,12-Tricosadiynoic acid and the phospholipids, dissolved in ethanol:chloroform 1:1, were mixed in a glass tube in 3:2 ratio (diacetylene:lipids) and dried *in vaccuo*. The resulting lipid film was hydrated with deionized water and sonicated using a Misonix Incorporated sonicator (Farmingdale, NY). The tubes were heated to 70 °C during the sonication process. The vesicle suspension was cooled to room temperature and incubated overnight at 4 °C followed by polymerization by UV irradiation at 254 nm for 20−30 s to create polydiacetylene (PDA).

2.7. PDA Fluorescence. PDA/phospholipid vesicles were mixed with various amounts of peptide followed by addition of Tris buffer and filled with water to 1 mL. Final concentrations: lipids 30 μM, Tris 1.5 mM, novicidin (3.48−0.435 μM; peptide:lipid ratio 1:8−1:70). The solution was transferred to a 1 mL quartz cuvette, and the fluorescence emission spectra were taken (530−700 nm) with the excitation wavelength 488 nm. Spectra were baselined, and the emission intensity at 560 nm was plotted as a function of the peptide concentration, creating a titration curve.

2.8. Tyrosine Fluorescence. Internal fluorescence of novicidin was measured in quartz cuvette (1 mL volume) using an FL-920 spectrofluorimeter (Edinburgh, U.K.). The excitation wavelength was set to 279 nm, emission spectra were taken from 295 to 360 nm, and each spectrum was corrected by baseline subtraction using the appropriate peptide-free liposome solution. The suspension of liposomes (1 mM total lipid concentration) was mixed with Tris buffer (final concentration 1.5 mM, pH 8), and then, the peptide was added. The volume was filled to 1 mL using deionized water. The novicidin concentration remained constant for all measurements (3.5 μM), and the peptide to lipid ratio (from approximately 1:2 to 1:60) was varied by changing the volume of added liposomes.

2.9. Circular Dichroism (CD). The vesicle suspension (1 mM) was mixed with the Tris buffer (50 mM, pH 8.0) first, and then, the peptide was added (2 mg/mL). Final concentrations used: Tris 5 mM, novicidin 0.1 mg/mL (43.5 μM), and lipids 435 μM. Peptide concentration was determined after the measurement using the BCA method. Solutions were placed into a demountable, quartz cuvette with 0.1 cm path length, and spectra were obtained using a Jasco J-815 CD spectrometer (Jasco Spectroscopic Co., Hachioji City, Japan) using the following settings: spectrum range 185−260 nm, scanning speed 10 nm/min, integration time 4 s, and data pitch 1 nm.

2.10. Electron Spin Resonance (ESR). Vesicles containing 2% of DOXYL probe were mixed with Tris buffer (pH 7.4) and the peptide (final concentrations: lipids 0.5 mM, Tris 25 mM, novicidin 14.3 μM). Samples were placed in a 20 mm length, 1 mm internal-diameter quartz capillary, and ESR spectra were recorded on a Bruker EMX-220 digital X-band spectrometer at room temperature. Amplitudes of 12.5 and 100 kHz, modulation, and microwave power level were selected at subcritical values (0.5 G and 20 mW, respectively) to obtain the best signal-to-noise ratio. Processing of the ESR spectra was carried out using Bruker WIN-EPR software.

TABLE 1: Antibacterial and Hemolytic Activities of Novicidin

	minimal inhibitory concentration (MIC, μM)			
compound	*E. coli* BL21	*S. enterica ser. Typhimurium*	*B. cereus*	hemolytic activity (IC50, μM)
novicidin	0.65 ± 0.3	1.4 ± 0.4	1.4 ± 1.0	>50
melittin	2.2 ± 0.7	0.4 ± 0.2	1.0 ± 0.5	1.6 ± 0.5
streptomycin	20 ± 7	86 ± 26	3.5 ± 1.7	n/a

The rotational correlation time was calculated according to the equation

$$\tau_c = 6.65 \cdot \Delta H_{+1}[(I_{+1}/I_{-1})^{1/2} - 1] \cdot 10^{-10} \quad \text{(s)}$$

where I_{+1}/I_{-1} corresponds to the amplitude of low- and high-field components and ΔH_{+1} is the width of the low-field component of the spectra.[20]

2.11. Monte Carlo (MC) Simulations. MC simulations of novicidin were performed according to methodologies described previously.[21−25] Novicidin was depicted in a reduced way, in which each amino acid was represented by two interaction sites, corresponding to the α-carbon and side chain. These interaction sites, as well as sequential α-carbons, were connected by virtual bonds. The hydrophobicity of the membrane was represented as a smooth profile of 30 Å width, corresponding to the hydrocarbon region of phosphatidylcholine (PC) and phosphatidylglycerol (PG) membranes. A negative surface charge was located on both sides of the membrane at a distance of 20 Å from the midplane. Its magnitude corresponded to the fraction of acidic lipids (0, 20, 50, and 100 mol %, in accordance with the experiments). The solution was considered neutral with monovalent salt at a concentration of 0.1 M. Novicidin's initial structure was modeled using the Scap methodology[26] and Protein Data Bank entry 1HU6[18] as a template. To calculate the free energy of the peptide in water and in the membrane, four simulations consisting of 900 000 Monte Carlo cycles were conducted. In the simulations in water, the peptide was subjected to internal conformational modifications only, while in the membrane simulations the peptide was additionally allowed to change its location and orientation relative to the membrane. The total free energy of membrane association was calculated as the difference between the free energies of the peptide in water and in the membrane. A detailed description of the energetic terms included can be found in the Supporting Information. The helical content of novicidin was calculated as described in ref 22.

3. Results

3.1. Biological Activity. Table 1 summarizes the hemolytic and antimicrobial properties of novicidin, evaluated by commonly used Gram-negative and Gram-positive bacterial species. For comparison, we also outline in Table 1 the hemolytic and antimicrobial properties of melittin, a widely studied cytolytic peptide,[27] and streptomycin, a conventional antibiotic.[28] The low minimal inhibitory concentrations (MICs) recorded for novicidin (Table 1) attest to its effective antibacterial properties. A recent study recording the antibacterial properties of novicidin against an array of *Listeria monocytogenes* and *Staphylococcus aureus* strains similarly reported low MICs for the peptide.[29] Table 1 also confirms the low hemolytic activity of novicidin; the recorded IC50 of the peptide (>50 μM) is significantly higher than that of melittin (1.6 μM).

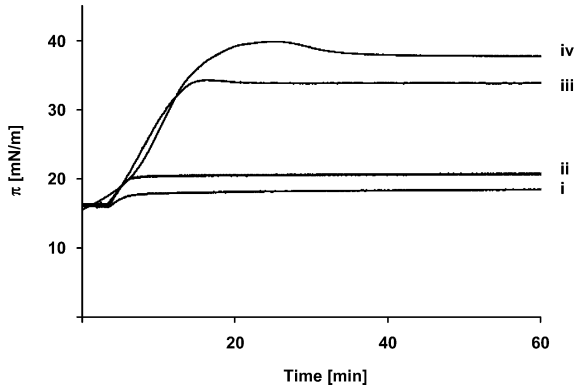

Figure 2. Isothermal adsorption of novicidin onto phospholipid monolayers. Adsorption isotherms of 87 nM novicidin injected under preformed phospholipid monolayers (initial monolayer pressure 16 mN/m): (i) DMPC; (ii) DMPC:DMPG 4:1; (iii) DMPC:DMPG 1:1; (iv) DMPG. The increase in the surface pressure of monolayers containing anionic phospholipids indicates enhanced penetration of the peptide into monolayers containing negative phospholipids. Almost no surface pressure change was recorded for the zwitterionic monolayer, indicating very weak interaction. The experimental sample size was $n = 2$.

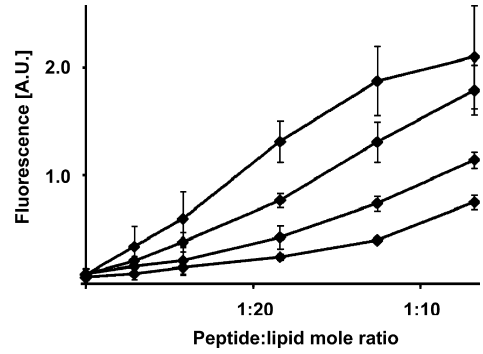

Figure 3. Fluorescence dose−response curves of lipid/PDA vesicles. Novicidin induces perturbations of phospholipid/PDA bilayer vesicles leading to induction of fluorescence emission at 560 nm. Differences in fluorescence emission in various lipid compositions are dependent upon the degree of penetration of the peptide: (i) DMPC:PDA 2:3 (mole ratio); (ii) DMPC:DMPG:PDA 1.6:0.4:3; (iii) DMPC:DMPG:PDA 1:1:3; (iv) DMPG:PDA 2:3. The experimental sample size was $n = 2$.

The biological (both hemolytic and antibacterial) activities of cationic AMPs are believed to be strongly associated with their *membrane interactions*.[9,30] We applied several biophysical techniques designed to characterize the binding and insertion of novicidin into model phospholipid membranes. The data, presented and discussed below, help to shed light on the likely mechanisms of antibacterial action and cell specificity of novicidin.

3.2. Biophysical Characterization. Figure 2 depicts isothermal adsorption experiments in which 87 nM novicidin was injected underneath lipid monolayers deposited at the air/water interface.[31] Langmuir monolayers of lipids have been widely employed as useful biomimetic assemblies;[32,33] in particular, numerous studies have focused on the analysis of peptide incorporation into lipid monolayers as models for peptide/membrane interactions.[34,35] The adsorption isotherms depicted in Figure 2 demonstrate the dramatic effect of the phospholipid headgroup charge upon novicidin adsorption and penetration into the lipid monolayers.

The adsorption isotherm in Figure 2,i shows a negligible increase in surface pressure following injection of novicidin underneath a monolayer comprising the zwitterionic phospholipid dimyristoylphosphatidylcholine (DMPC). This result indicates a minimal insertion of novicidin into the DMPC monolayer. Importantly, Figure 2 demonstrates that when the monolayer contained a higher concentration of dimyristoylphosphatidylglycerol (DMPG), a negatively charged phospholipid, more pronounced incorporation of novicidin within the monolayer occurred, giving rise to higher surface pressures. This observation highlights not only the pronounced affinity of the peptide to monolayers containing anionic lipids but particularly the fact that the peptide *inserted* into the DMPG-containing monolayers. Such interpretation is also consistent with our previous investigations indicating that novicidin adopts secondary structure elements allowing for lipid incorporation.[36]

While Figure 2 indicates that negatively charged DMPG significantly promotes insertion of novicidin into lipid monolayers at the air/water interface, additional experiments were carried out to evaluate the extent of insertion of the peptide into lipid bilayers, which is the actual organization of lipid molecules within physiological membranes. Figure 3 illustrates the application of a biomimetic lipid/polymer assay to explore the relationship between the extent of bilayer insertion and lipid composition. Specifically, Figure 3 presents fluorescence dose response curves recorded following incubation of novicidin with phospholipid/polydiacetylene (PDA) vesicles. PDA is a unique chromatic polymer which undergoes visible *blue−red* transformations as well as *fluorescence emission* induced by varied molecular interactions.[37] In particular, mixed vesicles comprising PDA and lipid molecules have been previously used for analysis of membrane interactions of antimicrobial peptides and other membrane-associated molecules.[37–39] In such lipid/PDA vesicle systems, interactions of membrane-active molecules resulting in disruption of the lipid bilayer led to significantly enhanced fluorescence emission from the associated PDA polymer matrix. Furthermore, the chromatic response of the vesicles can be employed to distinguish between *surface interactions* of tested peptides on the one hand and *subsurface insertion* on the other hand, based upon the relative *steepness* of the dose−response curves.[40]

Figure 3 depicts the effect of the anionic phospholipid DMPG in phospholipid/PDA vesicles on the mode of interaction of novicidin with the membrane. *Steeper* dose response curves were observed following incubation of novicidin with vesicles containing *less* DMPG. For example, 15 μM novicidin induced a relative fluorescence of 1.0 (arbitrary units, a.u.) in DMPC/PDA (2:3 mol ratio) vesicles (Figure 3,i), while the same concentration gave rise to less than 0.4 a.u. in a solution of DMPC/DMPG/PDA (1:1:3) vesicles (Figure 3,ii). These results can be explained according to the extent of novicidin interaction with the vesicle surface. In the DMPC/PDA biomimetic membrane, novicidin is most likely associated with the PDA headgroups (which are negatively charged), giving rise to the *steeper* dose response curve (Figure 3,i). In comparison, in vesicles containing more DMPG, a significant fraction of novicidin is probably immersed within the DMPG domains, overall leading to *less* surface perturbation of the PDA matrix and consequently giving rise to a more *moderate* curve compared to DMPC/PDA.

Previous studies have indicated that the fluorescence emission induced in lipid/PDA systems is ascribed to *surface perturbations* of the vesicles.[37] Accordingly, the fluorescence results in Figure 3 suggest that DMPG promotes *deeper insertion* of novicidin beyond the bilayer surface, giving rise to relatively lower fluorescence responses, while DMPC causes a higher degree of *surface binding* leading to higher chromatic response. Indeed, the most moderate fluorescence dose response curve

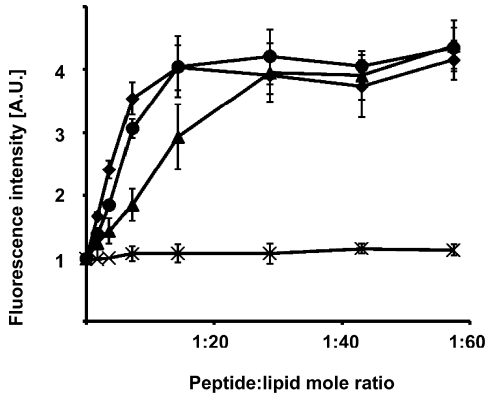

Figure 4. Tyrosine fluorescence titration curves. Titration with liposomes containing different ratios of DMPG vs DMPC. Novicidin interaction induces an increase of fluorescence emission at 304 nm (Y17) due to penetration of the peptide into the lipid bilayer. (×) DMPC; (▲) DMPC:DMPG (4:1 mol ratio); (●) DMPC:DMPG (1:1); (◆) DMPG. THe experimental sample size was $n = 6$.

was apparent when novicidin was incubated with DMPG/PDA vesicles (Figure 3,iv).

Tyrosine fluorescence data depicted in Figure 4 lend support to the interpretation of the chromatic lipid/PDA assay results, confirming that DMPG promoted more pronounced incorporation of novicidin into the bilayer. Aromatic amino acids such as tryptophane and tyrosine have been shown to localize preferentially at the membrane interface (headgroup region).[41,42] In particular, the fluorescence emission of tyrosine has been shown to exhibit pronounced sensitivity to the hydrophobicity of its microenvironment.[43] Indeed, Tyr fluorescence spectroscopy is regularly employed to evaluate the extent of peptide interactions with lipids.[44]

Novicidin has one Tyr residue in position 17. The tyrosine fluorescence titration data in Figure 4 confirm that novicidin did not penetrate into DMPC bilayers, yielding almost unchanged fluorescence emission as the lipid:peptide ratio increased (Figure 4, crosses). However, significantly higher fluorescence was recorded when novicidin was added to vesicles comprising, in addition to DMPC, also the negatively charged DMPG. Similar to the chromatic assay results in Figure 3, Figure 4 demonstrates that higher abundance of DMPG within the vesicles correlated with greater insertion of novicidin beyond the lipid/water interface. Indeed, the highest increase in tyrosine fluorescence emission was observed when novicidin was added to DMPC:DMPG (1:1 mol ratio) vesicles and to pure DMPG vesicles, respectively (Figure 4, filled circles and filled diamonds, respectively).

To corroborate the fluorescence data in Figures 3 and 4, which point to a direct relationship between DMPG content and bilayer insertion, and probe the approximate depth of peptide insertion into the bilayer, we further carried out electron spin resonance (ESR) spectroscopy experiments utilizing phospholipid vesicles which additionally included phosphatidylcholine displaying a doxyl spin probe in position 10 of the acyl chain (PC-10-DS, Table 2). Table 2 depicts the effect of novicidin upon the rotational correlation times of the doxyl residue, denoted τ_c, which are highly sensitive to the local dynamical properties of the spin-probe within the lipid bilayer.[45]

Table 2 demonstrates that addition of novicidin resulted in dramatic transformations of the τ_c values. Particularly important, changes of the rotational correlation times were clearly dependent upon the presence of DMPG in the vesicles. Specifically, in 10-DS-PC/DMPC (1:50 mol ratio) vesicles, incubation with

TABLE 2: ESR Data—Rotational Correlation Times, τ_c, of PC-10-DS Incorporated into the Phospholipid Vesicles[a]

	τ_c (ns)	
	control	novicidin
DMPC	2.63	2.73
DMPC:DMPG 4:1	2.21	3.79
DMPG	1.93	7.80

[a] SD values were less than 10%.

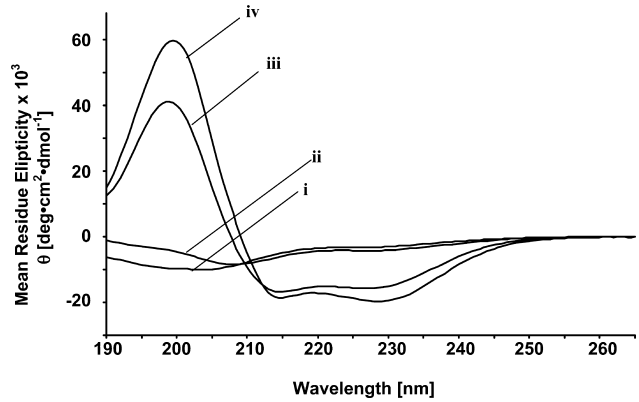

Figure 5. Circular dichroism (CD). Far UV CD spectra of novicidin in different environments: (i) Tris buffer; (ii) DMPC; (iii) DMPC:DMPG 4:1; (iv) DMPG. Novicidin adopts an α-helical structure when incubated with negatively charged liposomes (iii and iv), whereas it is unstructured in the buffer (i). The spectrum obtained for DMPC vesicles (ii) differs from the one in the buffer (i), exhibiting a higher signal in the region corresponding to a positive band characteristic for the α-helix and a slightly lower signal in the region corresponding to a negative band of the helical structure, indicating a minor structural change of the peptide.

novicidin yielded a minimal change to τ_c from 2.63 to 2.73 ns (Table 2), consistent with the proposed *surface localization* of novicidin in bilayers comprising only DMPC. However, almost a 2-fold increase in correlation time compared to the control vesicles, from 2.21 to 3.79 ns, was apparent when novicidin was added to 10-DS-PC/DMPC/DMPG (1:25:25) vesicles, and a 4-fold greater τ_c was recorded when the peptide was incubated with 10-DS-PC/DMPG (1:50) vesicles. The increase in τ_c is indicative of the slower mobility of the spin probes and underscores lower membrane fluidity.[46] Accordingly, since the doxyl residue in 10-DS-PC is localized closer to the middle of the lipid acyl chains, the τ_c data likely indicate that novicidin insertion into the headgroup/acyl chain interface affects the bilayer interior, possibly through penetration of the side-chains of hydrophobic residues, such as leucine and isoleucine, into the hydrocarbon region of the bilayer.

While Figures 2−4 and Table 2 highlight the relationship between novicidin membrane penetration and the abundance of the negatively charged phospholipid DMPG as compared to zwitterionic DMPC, we further assessed the consequences of membrane interactions upon the peptide *structure*. Figure 5 depicts circular dichroism (CD) spectra of novicidin incubated with different vesicle systems. In a buffer solution (no lipids present), the CD spectrum of novicidin (Figure 5,i) exhibits a pronounced dip at around 198 nm, indicative of a predominant random coil structure. The CD trace of novicidin incubated with DMPC vesicles (Figure 5,ii), although slightly different than the peptide in the buffer solution, similarly points to a highly disordered conformation of the peptide. It should be pointed out, however, that the CD spectra in buffer (Figure 5i) and in PC (Figure 5i) are different, especially in the region 190−205

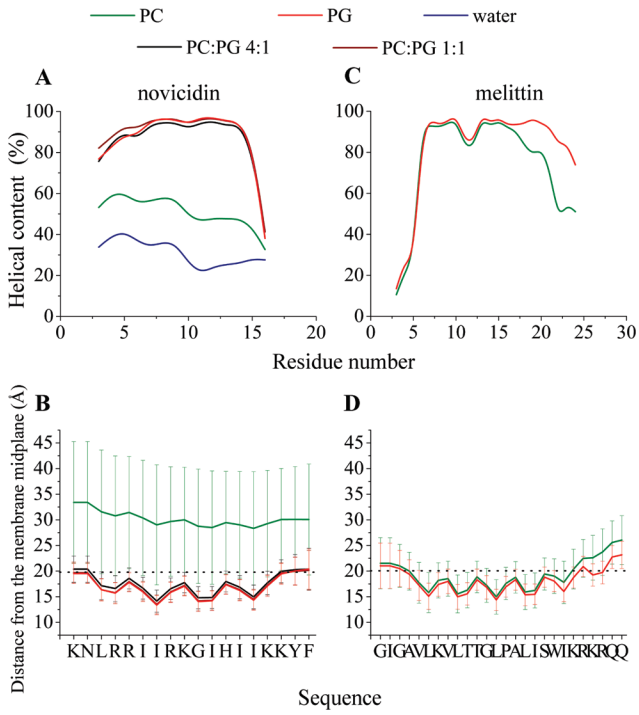

Figure 6. Peptide helicity and location of the α-carbon atoms in the lipid bilayer based on Monte Carlo simulations. The curves obtained for water solution and bilayers comprising different lipid compositions are depicted in different colors. (A, C) The calculated helical content of novicidin (A) and melittin (C) in the aqueous phase and lipid bilayers. (B, D) Average conformations of novicidin (B) and melittin (D) in the lipid bilayer determined as the average distance of each residue alpha-carbon from the bilayer midplane. The error bars mark the standard deviations. For clarity, the error bars of novicidin in DMPC:DMPG 1:1 and DMPC:DMPG 4:1 are omitted. The residues are indicated using a one-letter code. The horizontal dotted line marks the location of the phosphate group of the lipid polar heads.

nm. In PC, the signal is more positive (displaying a spectral maximum at around 195 nm) than in buffer. Furthermore, the minima at 208 and 222 nm (helix signature) are somewhat more pronounced in PC than in water. These differences are small but experimentally significant, and possibly point to a residual helical structure in the presence of DMPC vesicles.

The CD results reveal a dip at around 220 appearing in the spectra as the DMPG content in the vesicles gradually increased (Figure 5,iii−iv). CD traces featuring dips at around 208 and 222 nm generally point to the formation of a helical peptide conformation.[47] This result confirms the empirical prediction that the anionic membranes would induce the α-helical structure of novicidin. Indeed, many cationic AMPs exhibit a general tendency to adopt helical structures upon interactions with the negatively charged membranes.[6,30]

3.3. Monte Carlo Simulations. The results of Monte Carlo (MC) simulations, depicted in Figures 6 and 7, provide a computational chemistry framework for the experimental data and their interpretation. The calculated helical contents of novicidin in water and in bilayers of different lipid compositions correlate well with the CD spectra. Novicidin is, in essence, randomly coiled in water (Figure 6A). The helicity of novicidin only slightly increased due to the surface interaction with a neutral (DMPC) lipid bilayer and markedly increased with the addition of negatively charged lipids (DMPG) (Figure 6A). In comparison, melittin which is less charged and more hydrophobic exhibits high helicity both in the charged and neutral lipid bilayers (Figure 6C).

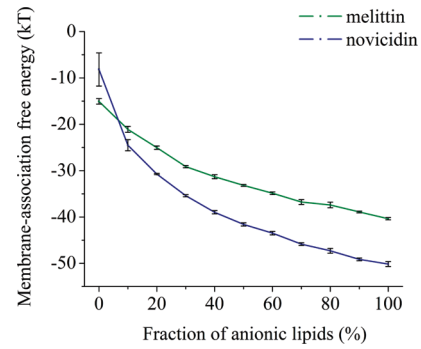

Figure 7. Calculated free energy of membrane association of novicidin (blue) and melittin (green) as a function of the fraction of anionic lipids in the bilayer. The error bars indicate the standard deviation. Please notice that for the most part the error bars are smaller than the marks of the data points.

The orientation of novicidin within bilayers of various lipid compositions was estimated on the basis of the average distances of the residues from the membrane midplane (Figure 6B). Figure 6B shows that in all cases the peptide backbone was approximately parallel to the bilayer surface. In a purely neutral membrane (corresponding to a DMPC lipid bilayer), novicidin interacted very weakly with the membrane (membrane-association free energy of about −8kT) and, for the most part, remained in the aqueous phase approximately 30 Å from the bilayer midplane (Figure 6B).

The incorporation of negative surface charge into the bilayer (the model's representation of the negatively charged DMPG lipids) led to penetration of novicidin into the headgroup region of the membrane. This location was favorable, since it enabled the hydrophobic residues to be buried in the hydrocarbon region of the membrane, while the positively charged residues interacted through Coulomb attraction with the negative membrane-surface charge. The charged and polar residues remained in the water−bilayer interface to minimize the desolvation penalty associated with their transfer into the hydrophobic region of the membrane. A similar conformation was previously described for melittin[24] (Figure 6D), as well as for NKCS and two derivatives.[25] In addition, the position of the tyrosine residue (Tyr-17) at the membrane interface region is in agreement with previous reports.[41,42] However, in contrast to melittin, novicidin did not partition into the polar headgroup region in a pure PC membrane and its penetration was dependent on the presence of the negatively charged lipids. This property was manifested also by NKCS and its two derivatives.[25] Figure 6B also points to the greater flexibility of the *C-terminus* of the peptide (e.g., larger error bars), likely induced by electrostatic repulsion between asparagine and the negatively charged phospholipids in the bilayer.

Figure 7 confirms that the membrane-association free energy of novicidin increased with the fraction of negatively charged lipids. It also shows a comparison of the novicidin data with previous simulations of melittin within bilayers of different compositions.[24] In both cases, the calculated free energy values correlated well with the experimentally estimated hemolytic and antibiotic activity data (Table 1). Novicidin's MIC against bacteria is comparable to the MIC of melittin (Table 1). This observation correlates with the similar penetration depth of both peptides into negatively charged membranes, despite novicidin's lower (more favorable) binding free energy to the negatively charged lipids, relative to melittin (Figure 6D). Although the association energy of melittin to negatively charged membranes is higher than that of novicidin, it is still low enough to

effectively bind, and penetrate bacterial membranes (containing 20−40% of anionic lipids for Gram-negative bacteria and up to 100% negatively charged lipids for Gram-positive bacteria[48]) at the concentrations used. Likewise, the higher (less favorable) free energy of novicidin association with the neutral bilayer could be ascribed to its lower hemolytic activity in comparison to melittin. Moreover, the average conformations of novicidin and melittin within a neutral lipid bilayer support this notion (Figure 6B and D). While melittin was immersed within the uncharged bilayer, novicidin remained only loosely associated with the membrane's surface.

4. Discussion

A primary question pertaining to the biological activity of novicidin concerns the factors affecting its significant antimicrobial activity on the one hand and diminished hemolytic action on the other hand. The experimental data and MC simulations provide a framework for understanding both cell selectivity and bacterial toxicity. In particular, our results point to the role of negatively charged lipids, specifically phosphatidylglycerol, as determining membrane insertion of novicidin.

The data presented here underscore a significant effect of negatively charged phospholipids upon binding and insertion of novicidin into membrane bilayers. Indeed, the presence of DMPG was found to constitute an essential prerequisite for novicidin attachment and penetration into lipid bilayers. This observation, combined with the lack of helical structure and negligible insertion of novicidin into pure zwitterionic lipid bilayers, might explain the selectivity of the peptide toward bacterial cells, which generally display a much higher abundance of negatively charged phospholipids in their membranes.[48] Diminished membrane interactions of AMPs with zwitterionic lipids have been widely observed and are believed to account for their low hemolytic activities.[49,50] Similarly, binding of cationic AMPs to negatively charged lipids has been reported in varied membrane systems mimicking bacterial membranes.[51,52]

The differences between melittin and novicidin both in the biological context (Table 1) as well as the MC calculations pertaining to membrane localization (Figure 6) are noteworthy. Specifically, the ability of melittin to insert into zwitterionic membranes and consequent hemolytic activity most likely emanates from its specific distribution of hydrophobic and positively charged residues in the sequence and its overall hydrophobicity. These properties are reflected in the lower (more negative) energy of melittin association with neutral membranes compared to novicidin. Melittin contains five positively charged residues, mostly clustered at the N-terminus, and 11 hydrophobic residues (I, L, V, F, and A). Novicidin, on the other hand, has seven cationic residues distributed evenly along the peptide and seven hydrophobic residues. The higher portion of hydrophobic amino acids presumably assures melittin's interaction with zwitterionic membranes.

Interestingly, ovispirin, another peptide that has the same ratio of hydrophobic vs charged amino acids as novicidin, exhibits high hemolytic and cytotoxic properties.[18] Indeed, our MC simulations showed that ovispirin associates with neutral lipids (Supporting Information, Figure S1A). The differences between the novicidin and ovispirin constitute Gly vs Ile at position 10 and Phe vs Gly at position 18. Roughly speaking, these substitutions preserve the overall hydrophobicity level of the peptide. However, the effect of the substitution in position 10 is more pronounced, since it is much closer to the membrane than position 18. The important role of the G10I substitution is further supported by another close relative: the novispirin peptide which has only one of the two substitutions, F18G. The MC simulations, as well as experimental data,[18] showed that novispirin has a weak affinity for and does not insert into a neutral bilayer (Supporting Information, Figure S1B).

Further to these arguments, it has been suggested that hemolysis of eukaryotic cells by AMPs is not solely dependent on the electrostatic attraction to the membrane but requires peptide penetration into the hydrophobic core of the membrane and simultaneous α-helix formation.[6,30] An interesting example demonstrating this phenomenon is dermaseptin B2, which adopts a helical structure in zwitterionic membranes and is therefore highly cytolytic. A variant of dermaseptin lacking the hydrophobic C-terminal part (crucial for adopting a helical conformation in zwitterionic membranes) remains unordered in phosphatidylcholine vesicles and, more significantly, has very low cytolytic properties.[53] A recent study on the cationic peptide pardaxin has demonstrated a dependence of the secondary structure and the mode of action upon membrane composition.[54] Pardaxin adopted a helical conformation in zwitterionic DOPC vesicles and permeabilized the bilayer through a "barrel-stave" mechanism, whereas in anionic vesicles (DOPC/PG) the peptide disrupted the membrane via the "carpet" mechanism. The ability of pardaxin to form an α-helix in zwitterionic membranes is likely to be the key to the cytolytic activity, since its diastereoisomer, which is unable to adopt a helical conformation, is nonhemolytic.[55] Unlike the cytolytic peptide pardaxin, novicidin *did not* adopt a helical structure upon interaction with zwitterionic membranes (Figures 5,ii and 6A) and did not penetrate into the bilayer (Figures 2−4). This conclusion accounts for novicidin's very low hemolytic activity (Table 1).

In addition to modulation of the membrane specificity of novicidin, the experiments point to an important role of negatively charged phospholipids in promoting insertion of novicidin into the interface between the hydrophilic headgroups and the hydrophobic tails of the lipids. The incorporation of novicidin within DMPG-containing bilayers was evident through application of the biophysical techniques employed, including the chromatic lipid/PDA assay (Figure 2), tyrosine fluorescence (Figure 3), and ESR (Table 2). Folding of novicidin into a pronounced helical conformation upon interaction with DMPG vesicles (Figures 4 and 5B) provides a structural framework for insertion of the peptide into the bilayer, rather than localization only at the lipid/water interface.

Insertion of novicidin into the headgroup region, promoted by negatively charged phospholipids and a serious membrane perturbation, may well be the underlying mechanism for the antibacterial action of the peptide. Subsurface bilayer penetration has been previously observed for some cationic peptides.[56,57] In conclusion, this investigation reveals the critical role of the phospholipid headgroup charge in determining the biological activity of novicidin, a novel antimicrobial peptide, particularly as the molecular determinant for discrimination between mammalian and bacterial membranes.

Acknowledgment. This research project has been supported by the European Commission under the sixth Framework Program through the Marie-Curie Action: BIOCONTROL, contract number MCRTN − 33439. We are grateful to Dr. Hans Henrik Kristensen for providing novicidin. Support from the Danish National Research Foundation is also acknowledged.

Supporting Information Available: Details of energy calculations for the Monte Carlo simulations are presented as well as the location of novispirin and ovispirin peptides in

neutral lipid membranes. This material is available free of charge via the Internet at http://pubs.acs.org.

References and Notes

(1) Zasloff, M. *Nature* **2002**, *415*, 389–395.
(2) Bulet, P.; Stöcklin, R.; Menin, L. *Immunol. Rev.* **2004**, *198*, 169–184.
(3) Hancock, R. E.; Diamond, G. *Trends Microbiol.* **2000**, *8*, 402–410.
(4) Yount, N. Y.; Bayer, A. S.; Xiong, Y. Q.; Yeaman, M. R. *Biopolymers* **2006**, *84*, 435–458.
(5) Brown, K. L.; Hancock, R. E. W. *Curr. Opin. Immunol.* **2006**, *18*, 24–30.
(6) Jiang, Z.; Vasil, A. I.; Hale, J. D.; Hancock, R. E. W.; Vasil, M. L.; Hodges, R. S. *Biopolymers* **2008**, *90*, 369–383.
(7) Rotem, S.; Mor, A. *Biochim. Biophys. Acta* **2009**, *1788*, 1582–1592.
(8) Matsuzaki, K. *Biochim. Biophys. Acta* **1999**, *1462*, 1–10.
(9) Shai, Y. *Biochim. Biophys. Acta* **1999**, *1462*, 55–70.
(10) He, K.; Ludtke, S. J.; Huang, H. W.; Worcester, D. L. *Biochemistry* **1995**, *34*, 15614–15618.
(11) Oren, Z.; Shai, Y. *Biopolymers* **1998**, *47*, 451–463.
(12) Matsuzaki, K.; Murase, O.; Fujii, N.; Miyajima, K. *Biochemistry* **1996**, *35*, 11361–11368.
(13) Ludtke, S. J.; He, K.; Heller, W. T.; Harroun, T. A.; Yang, L.; Huang, H. W. *Biochemistry* **1996**, *35*, 13723–13728.
(14) Huang, H. W. *Biochemistry* **2000**, *39*, 8347–8352.
(15) Bechinger, B.; Lohner, K. *Biochim. Biophys. Acta* **2006**, *1758*, 1529–1539.
(16) Dittmer, J.; Thøgersen, L.; Underhaug, J.; Bertelsen, K.; Vosegaard, T.; Pedersen, J. M.; Schiøtt, B.; Tajkhorshid, E.; Skrydstrup, T.; Nielsen, N. C. *J. Phys. Chem. B* **2009**, *113*, 6928–6937.
(17) Bertelsen, K.; Paaske, B.; Thøgersen, L.; Tajkhorshid, E.; Schiøtt, B.; Skrydstrup, T.; Nielsen, N. C.; Vosegaard, T. *J. Am. Chem. Soc.* **2009**, *131*, 18335–18342.
(18) Sawai, M. V.; Waring, A. J.; Kearney, W. R.; McCray, P. B. J.; Forsyth, W. R.; Lehrer, R. I.; Tack, B. F. *Protein Eng.* **2002**, *15*, 225–232.
(19) Wimmer, R.; Andersen, K. K.; Vad, B.; Davidsen, M.; Mølgaard, S.; Nesgaard, L. W.; Kristensen, H. H.; Otzen, D. E. *Biochemistry* **2006**, *45*, 481–497.
(20) Freed, J. H.; Fraenkel, G. K. *J. Chem. Phys.* **1963**, *39*, 326–348.
(21) Kessel, A.; Shental-Bechor, D.; Haliloglu, T.; Ben-Tal, N. *Biophys. J.* **2003**, *85*, 3431–3444.
(22) Shental-Bechor, D.; Kirca, S.; Ben-Tal, N.; Haliloglu, T. *Biophys. J.* **2005**, *88*, 2391–2402.
(23) Shental-Bechor, D.; Haliloglu, T.; Ben-Tal, N. *Biophys. J.* **2007**, *93*, 1858–1871.
(24) Gordon-Grossman, M.; Gofman, Y.; Zimmermann, H.; Frydman, V.; Shai, Y.; Ben-Tal, N.; Goldfarb, D. *J. Phys. Chem. B* **2009**, *113*, 12687–12695.
(25) Gofman, Y.; Linser, S.; Rzeszutek, A.; Shental-Bechor, D.; Funari, S. S.; Ben-Tal, N.; Willumeit, R. *J. Phys. Chem. B* **2010**, *114*, 4230–4237.
(26) Xiang, Z.; Honig, B. *J. Mol. Biol.* **2001**, *311*, 421–430.
(27) Blondelle, S. E.; Houghten, R. A. *Biochemistry* **1991**, *30*, 4671–4678.
(28) Berkman, S.; Henry, R. J.; Housewright, R. D. *J. Bacteriol.* **1947**, *53*, 567–574.
(29) Gottlieb, C. T.; Thomsen, L. E.; Ingmer, H.; Mygind, P. H.; Kristensen, H.; Gram, L. *BMC Microbiol.* **2008**, *8*, 205.
(30) Chen, Y.; Guarnieri, M. T.; Vasil, A. I.; Vasil, M. L.; Mant, C. T.; Hodges, R. S. *Antimicrob. Agents Chemother.* **2007**, *51*, 1398–1406.
(31) Maget-Dana, R. *Biochim. Biophys. Acta* **1999**, *1462*, 109–140.
(32) Brockman, H. *Curr. Opin. Struct. Biol.* **1999**, *9*, 438–443.
(33) Brezesinski, G.; Möhwald, H. *Adv. Colloid Interface Sci.* **2003**, *100−102*, 563–584.
(34) Vié, V.; Van Mau, N.; Chaloin, L.; Lesniewska, E.; Le Grimellec, C.; Heitz, F. *Biophys. J.* **2000**, *78*, 846–856.
(35) Volinsky, R.; Kolusheva, S.; Berman, A.; Jelinek, R. *Biochim. Biophys. Acta* **2006**, *1758*, 1393–1407.
(36) Vad, B.; Thomsen, L. A.; Bertelsen, K.; Franzmann, M.; Pedersen, J. M.; Nielsen, S. B.; Vosegaard, T.; Valnickova, Z.; Skrydstrup, T.; Enghild, J. J.; et al. *Biochim. Biophys. Acta* **2010**, *1804*, 806–820.
(37) Kolusheva, S.; Shahal, T.; Jelinek, R. *Biochemistry* **2000**, *39*, 15851–15859.
(38) Katz, M.; Tsubery, H.; Kolusheva, S.; Shames, A.; Fridkin, M.; Jelinek, R. *Biochem. J.* **2003**, *375*, 405–413.
(39) Satchell, D. P.; Sheynis, T.; Shirafuji, Y.; Kolusheva, S.; Ouellette, A. J.; Jelinek, R. *J. Biol. Chem.* **2003**, *278*, 13838–13846.
(40) Sheynis, T.; Sykora, J.; Benda, A.; Kolusheva, S.; Hof, M.; Jelinek, R. *Eur. J. Biochem.* **2003**, *270*, 4478–4487.
(41) Wimley, W. C.; White, S. H. *Nat. Struct. Biol.* **1996**, *3*, 842–848.
(42) Yau, W. M.; Wimley, W. C.; Gawrisch, K.; White, S. H. *Biochemistry* **1998**, *37*, 14713–14718.
(43) Giancotti, V.; Quadrifoglio, F.; Cowgill, R. W.; Crane-Robinson, C. *Biochim. Biophys. Acta* **1980**, *624*, 60–65.
(44) Lerche, M. H.; Kragelund, B. B.; Bech, L. M.; Poulsen, F. M. *Structure* **1997**, *5*, 291–306.
(45) Takahashi, T.; Noji, S.; Erbe, E. F.; Steere, R. L.; Kon, H. *Biophys. J.* **1986**, *49*, 403–410.
(46) Viriyaroj, A.; Kashiwagi, H.; Ueno, M. *Chem. Pharm. Bull.* **2005**, *53*, 1140–1146.
(47) Johnson, W. C. J. *Annu. Rev. Biophys. Biophys. Chem.* **1988**, *17*, 145–166.
(48) Epand, R. M.; Epand, R. F. *Biochim. Biophys. Acta* **2009**, *1788*, 289–294.
(49) Gazit, E.; Boman, A.; Boman, H. G.; Shai, Y. *Biochemistry* **1995**, *34*, 11479–11488.
(50) Dathe, M.; Meyer, J.; Beyermann, M.; Maul, B.; Hoischen, C.; Bienert, M. *Biochim. Biophys. Acta* **2002**, *1558*, 171–186.
(51) Matsuzaki, K.; Harada, M.; Funakoshi, S.; Fujii, N.; Miyajima, K. *Biochim. Biophys. Acta* **1991**, *1063*, 162–170.
(52) Abraham, T.; Lewis, R. N. A. H.; Hodges, R. S.; McElhaney, R. N. *Biochemistry* **2005**, *44*, 11279–11285.
(53) Joanne, P.; Galanth, C.; Goasdoué, N.; Nicolas, P.; Sagan, S.; Lavielle, S.; Chassaing, G.; El Amri, C.; Alves, I. D. *Biochim. Biophys. Acta* **2009**, *1788*, 1772–1781.
(54) Vad, B. S.; Bertelsen, K.; Johansen, C. H.; Pedersen, J. M.; Skrydstrup, T.; Nielsen, N. C.; Otzen, D. E. *Biophys. J.* **2010**, *98*, 576–585.
(55) Shai, Y.; Oren, Z. *J. Biol. Chem.* **1996**, *271*, 7305–7308.
(56) Breukink, E.; van Kraaij, C.; van Dalen, A.; Demel, R. A.; Siezen, R. J.; de Kruijff, B.; Kuipers, O. P. *Biochemistry* **1998**, *37*, 8153–8162.
(57) Christiaens, B.; Symoens, S.; Verheyden, S.; Engelborghs, Y.; Joliot, A.; Prochiantz, A.; Vandekerckhove, J.; Rosseneu, M.; Vanloo, B. *Eur. J. Biochem.* **2002**, *269*, 2918–2926.

JP1052248